

# $^{235}\text{U}$ nuclear relaxation rates in an itinerant antiferromagnet $\text{USb}_2$

S.-H. Baek,<sup>1</sup> N. J. Curro,<sup>2</sup> H. Sakai,<sup>1,3</sup> E. D. Bauer,<sup>1</sup> J. C. Cooley,<sup>1</sup> and J. L. Smith<sup>1</sup>

<sup>1</sup>*Los Alamos National Laboratory, Los Alamos, New Mexico 87545, USA*

<sup>2</sup>*Department of Physics, University of California, Davis, California 95616, USA*

<sup>3</sup>*Advanced Science Research Center, Japan Atomic Energy Agency, Tokai, Ibaraki 319-1195, Japan*

(Dated: March 8, 2019)

$^{235}\text{U}$  nuclear spin-lattice ( $T_1^{-1}$ ) and spin-spin ( $T_2^{-1}$ ) relaxation rates in the itinerant antiferromagnet  $\text{USb}_2$  are reported as a function of temperature in zero field. The heating effect from the intense rf pulses that are necessary for the  $^{235}\text{U}$  NMR results in unusual complex thermal recovery of the nuclear magnetization which does not allow measuring  $T_1^{-1}$  directly. By implementing an indirect method, however, we successfully extracted  $T_1^{-1}$  of the  $^{235}\text{U}$ . We find that the temperature dependence of  $T_1^{-1}$  for both  $^{235}\text{U}$  and  $^{121}\text{Sb}$  follows the power law ( $\propto T^n$ ) with the small exponent  $n = 0.3$  suggesting that the same relaxation mechanism dominates the on-site and the ligand nuclei, but an anomaly at 5 K was observed, possibly due to the change in the transferred hyperfine coupling on the Sb site.

## I. INTRODUCTION

In actinide-based materials,  $5f$ -electrons often exhibit itinerant and localized behavior simultaneously, which is in contrast to the usually localized  $4f$  electrons in the rare earth compounds. The unique nature of the  $5f$  electrons has been known to be the origin of various unusual physical properties found in actinide based materials such as unconventional superconductivity, non-Fermi liquid behavior, and multipolar ordering. However, since the degree of the  $5f$  localization is highly sensitive to the specific ligand atoms and the crystal structure, the nature of  $5f$  electrons is not easily elucidated even in a single compound.

In principle, nuclear magnetic resonance (NMR) is an ideal method to investigate  $5f$  electrons by probing on-site actinide nuclei ( $^{235}\text{U}$ ,  $^{237}\text{Np}$ ,  $^{239}\text{Pu}$ ) since they are directly influenced by  $5f$  electrons both dynamically and statically. However, NMR in the actinide nuclei is extremely difficult. For  $^{235}\text{U}$ , for instance, the tiny nuclear gyromagnetic ratio  $\gamma_n = 0.784$  MHz/T and very low natural abundance (0.72%) present significant challenges for detecting the NMR. Furthermore, the fast spin fluctuations of the  $5f$  electrons require an ordered state in which the spin fluctuations are sufficiently suppressed to allow the detection of NMR signal. Despite these difficulties,  $^{235}\text{U}$  NMR was successfully carried out recently<sup>1,2</sup> in an insulating  $\text{UO}_2$  and an itinerant  $\text{USb}_2$  in their antiferromagnetically ordered states. While  $^{235}\text{U}$  nuclear relaxation rates were measured in detail in  $\text{UO}_2$ , these quantities were not measured in  $\text{USb}_2$  that is highly itinerant. Motivated by the absence of  $T_1^{-1}$  in metallic U-based materials, we investigated the  $^{235}\text{U}$  nuclear relaxation rates in  $\text{USb}_2$ .

$\text{USb}_2$  is a member of the uranium dipnictides,  $\text{UX}_2$  family ( $X = \text{P, As, Sb, Bi}$ ), which is characterized by strong magnetic and electronic anisotropies, and the hybridization of the  $5f$  electrons with the conduction electrons.<sup>3,4,5,6</sup>  $\text{USb}_2$  crystallizes in the tetragonal  $\text{Cu}_2\text{Sb}$  type structure (space group:  $P4/nmm$ ) and undergoes

antiferromagnetic transition at  $T_N = 203$  K with an ordered moment of  $1.88 \mu_B$ .<sup>7</sup> The magnetic unit cell is doubled along the  $c$ -axis with respect to the chemical unit cell due to the sequence of alternating FM layers ( $\uparrow\downarrow\downarrow\uparrow$ ), as depicted in Fig. 1. dHvA experiment<sup>8</sup> detected the two-dimensional Fermi surfaces which are in agreement with the band calculations,<sup>6</sup> and the dual nature of the  $5f$  electrons was confirmed by ARPES study<sup>9</sup> from very narrow strongly dispersive bands at the Fermi level with  $5f$  character.

In this paper, we report the  $^{235}\text{U}$  nuclear spin-lattice ( $T_1^{-1}$ ) and spin-spin ( $T_2^{-1}$ ) relaxation rates in  $^{235}\text{U}$  enriched  $\text{USb}_2$  in an itinerant U-based compound,  $\text{USb}_2$ .

## II. SAMPLE PREPARATION AND EXPERIMENTAL DETAILS

We have grown single crystals of  $\text{USb}_2$  enriched with  $^{235}\text{U}$  (93.5 % enrichment) using flux growth in excess Sb. The  $^{235}\text{U}$  was arc-melted prior to the flux growth to remove the high vapor pressure daughters, radium in particular. Most of the  $\text{USb}_2$  produced was in the form of a single crystal weighing approximately 340 mg. Because the rf penetration depth is small an increase in signal strength can be accomplished by powdering the sample. The crystal was broken into pieces and  $\sim 100$  mg of material was ground into powder using an agate mortar and pestle. A pickup coil with an inside diameter of  $\sim 2$  mm was cast into an epoxy block and after curing a cylindrical sample space was drilled into the epoxy within the ID of the pickup coil. A 2 micron pore size stainless steel frit was glued over one end of the sample space. The  $\text{USb}_2$  powder was funneled into the open end of the sample space and a then a second frit glued on to close the open end. The frits allow thermal contact of the powder with the cryogenic fluid/gas and prevent the radioactive material from spreading into the apparatus.

$^{235}\text{U}$  and  $^{121}\text{Sb}$  NMR were performed in zero field in the temperature range 1.5–80 K. The NMR spectra were obtained by integrating averaged spin echo signals as

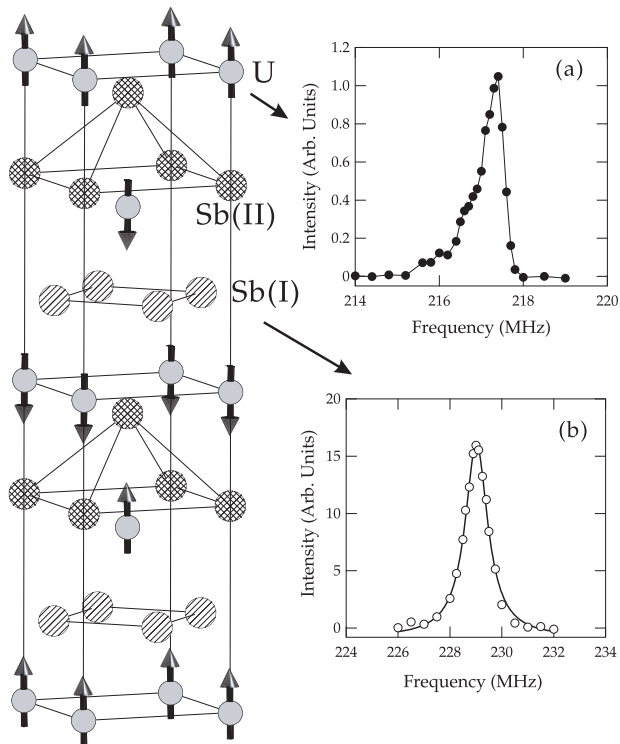


FIG. 1: The crystallographic and magnetic structure of  $\text{USb}_2$ . Arrows indicate the direction of the ordered moments along  $c$ -axis. Ferromagnetic planes are coupled ferromagnetically through Sb(I) plane but antiferromagnetically through Sb(II) plane. (a)  $^{235}\text{U}$  NMR spectrum and (b) second satellite spectrum of  $^{121}\text{Sb(I)}$  in zero field.

a function of frequency, and the spin-lattice relaxation rates ( $T_1^{-1}$ ) were measured by acquiring Hahn echoes following various delays after a saturation pulse. In order to extract  $T_1$ , we fit the raw data with the appropriate relaxation functions. The value of the nuclear spin-spin relaxation rate ( $T_2^{-1}$ ) was obtained by monitoring the spin-echo amplitude,  $M(2\tau)$ , as a function of  $2\tau$  between the first pulse and the echo. The  $M(2\tau)$  were fitted to an exponential decay curve  $M(0) \exp(-2\tau/T_2)$ .

### III. EXPERIMENTAL RESULTS AND DISCUSSION

From the detailed spectra of  $^{121,123}\text{Sb}$  and  $^{235}\text{U}$  given in ref. 2, we were able to confirm  $^{235}\text{U}$  signal at 217.4 MHz and the second satellite transition ( $5/2 \leftrightarrow 3/2$ ) of  $^{121}\text{Sb(I)}$  at 229 MHz as shown in Fig. 1 (a) and (b). While  $^{121}\text{Sb}$  spectrum has a Lorentzian shape, the U spectrum is asymmetric with shoulders in low frequency side. Since there is only one U crystallographic site in the unit cell, we suggest that a transferred hyperfine coupling from nearest neighbor U sites may lead to different inequivalent U sites in the complex magnetic structure. Indeed, the alternating ferromagnetic U planes suggest that dif-

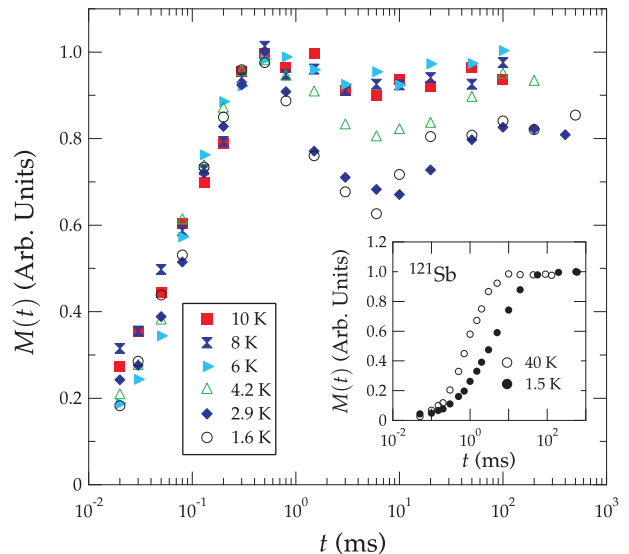


FIG. 2: Recovery of nuclear magnetization  $M(t)$  as a function of time  $t$  with varying temperature  $T$ .  $M(t)$  shows an oscillating behavior with varying  $t$ , forming a local minimum near  $t = 5$  ms. For  $t < 1$  ms,  $M(t)$  is almost independent of  $T$ , while the local minimum becomes deeper with decreasing temperature maintaining the same position in time. INSET: For comparison, the recovery curves for  $^{121}\text{Sb}$  are shown.

ferent transferred hyperfine coupling may result from the different interlayer magnetic interactions either through Sb(I) plane or Sb(II) plane. We will not present further analysis of this complicated  $^{235}\text{U}$  spectrum in this paper and, instead, we focus on the nuclear relaxation rates of  $^{235}\text{U}$ , which have never been directly measured in an itinerant magnetic material.

#### A. Thermal recovery of $^{235}\text{U}$ nuclear magnetization

As we try to measure  $^{235}\text{T}_1^{-1}$ , it turns out that the recovery of the nuclear magnetization,  $M(t)$ , is very unusual as shown in Fig. 2. With our experimental conditions, we were unable to make the full saturation of the line and there are always sizable signal more than 20 % with regard to the full amplitude. Also  $M(t)$  as a function of temperature  $T$  does not change below  $t < 0.5$  ms but it reveals an oscillating behavior with the minimum near  $t = 5$  ms. With decreasing  $T$ , the minimum becomes deeper without the change of its position in  $t$ .

We speculate that the unusual behavior of  $M(t)$  is due to the strong rf pulse in the sample coil, which may produce considerable heat causing complex thermal recovery of the nuclear magnetization. To flip a nuclear spin, we apply a  $\pi/2$  pulse that satisfies the relation  $\gamma_n H_1 \tau = \pi/2$ , where  $H_1$  corresponds to the rf strength (power) and  $\tau$  the duration of the pulse. Since  $\gamma_n = 0.784$  MHz/T of  $^{235}\text{U}$  is one order of magnitude smaller than typical nuclei (e.g., 10.189 MHz/T for  $^{121}\text{Sb}$ ), the total energy transferred to the coil,  $H_1 \tau$ , should be large correspondingly.

Moreover, the cooling power is substantially reduced in the measurement since the sample is located inside an epoxy block to prevent the contamination. Thus, the heating effect may be a consequence from the experimental limitations with regard to the  $^{235}\text{U}$  nuclei.

In order to account for the heating effect, we measured two data sets with different experimental conditions. One is measured through the usual sequence for measuring  $T_1$ . In an other sequence, we apply the saturating  $\pi/2$  pulse at off-resonance frequency  $\omega_{\text{off}}$  as depicted in the inset of Fig. 3 (a). The detecting pulses consisting of  $\pi/2 - \pi$  are the same in both sequences. Here, the  $Q$ -factor of the tank circuit is ensured to be low enough to cover  $\omega_{\text{off}}$  so that the rf power applied at  $\omega_{\text{off}}$ ,  $(\pi/2)_{\text{off}}$ , is fully transferred to the sample coil producing the similar amount of heat as the rf pulse applied at the resonance frequency  $\omega_{\text{on}}$ . If there is no heating effect, the second pulse sequence with  $(\pi/2)_{\text{off}}$  should give rise to a constant magnetization  $M(t) = M_0$ , since the  $(\pi/2)_{\text{off}}$  pulse does not flip the nuclei. Using this procedure, the thermal recovery of the magnetization  $M(t)_{\text{therm}}$  oscillates in a similar fashion with the total recovery of the magnetization  $M(t)_{\text{tot}}$  as shown in Fig. 3 (a).

We treat  $M(t)_{\text{therm}}$  as the fully recovered constant value  $M_0$  at each time so that the nuclear relaxation function can be written as

$$R(t) = 1 - M(t)_{\text{tot}}/M(t)_{\text{therm}}. \quad (1)$$

This accounts for not only the heating effect inside the sample coil but also any possible artificial effect originating from the power amplifier or the receiver. The corrected relaxation data are shown in Fig. 3 (b), and we fit the data with the relaxation function for the central transition of  $I = 7/2$  (solid lines),

$$R(t) = \frac{1}{84} \exp\left(-\frac{t}{T_1}\right) + \frac{3}{44} \exp\left(-\frac{6t}{T_1}\right) + \frac{75}{364} \exp\left(-\frac{15t}{T_1}\right) + \frac{1225}{1716} \exp\left(-\frac{28t}{T_1}\right). \quad (2)$$

### B. Nuclear relaxation rates, $T_1^{-1}$ and $T_2^{-1}$

The  $^{235}\text{U}$  nuclear spin-lattice relaxation rate  $^{235}T_1^{-1}$  as a function of temperature is shown in Fig. 4 (a). The data can be fit by a power law  $T^{0.3}$  in the measured temperature range.  $^{121}\text{Sb}$  nuclear spin-lattice relaxation rate  $^{121}T_1^{-1}$  also shows the same power law behavior with a factor of 4 smaller prefactor than that of  $^{235}T_1^{-1}$ . In general,  $T_1^{-1}$  due to the spin fluctuations is given by<sup>10</sup>

$$T_1^{-1} \approx 2T\gamma_n^2 A_{\text{hf}}^2 \frac{\sum_q \chi''_{\perp}(q, \omega_0)}{\omega_0}, \quad (3)$$

where  $A_{\text{hf}}$  is the hyperfine coupling constant at  $q = 0$ ,  $\chi''_{\perp}$  is the imaginary part of the  $q$ -dependent dynamic susceptibility at the nuclear Larmor frequency  $\omega_0$  that represents the spin fluctuations in the perpendicular plane.

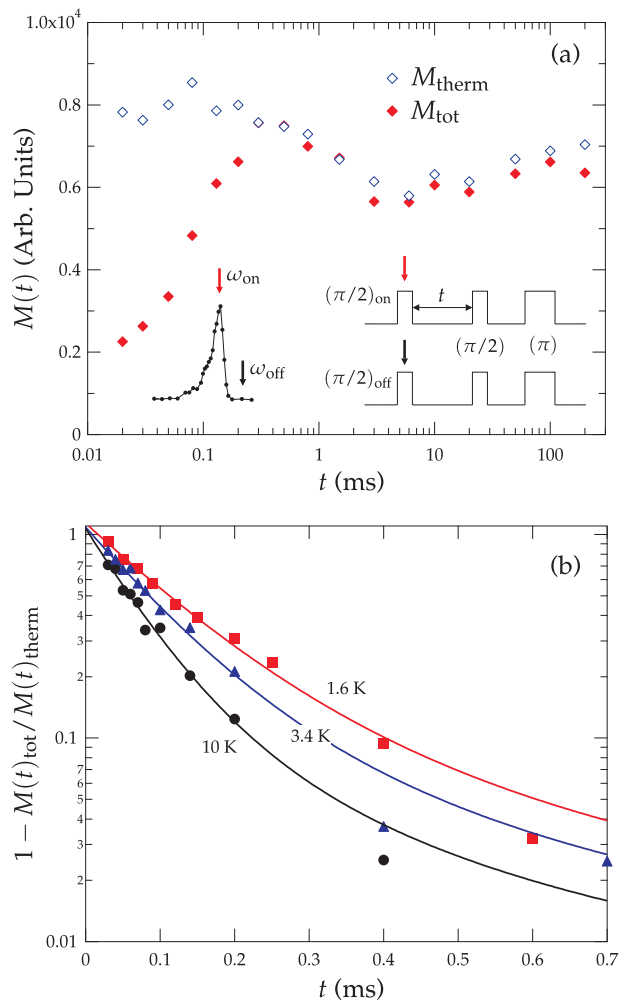


FIG. 3: (a) Total and thermal magnetization  $M(t)_{\text{tot}}$  and  $M(t)_{\text{therm}}$ , respectively. For  $M_{\text{tot}}$ , the typical pulse sequence for measuring  $T_1$  was used (upper diagram in inset). For  $M_{\text{therm}}$ , a saturating  $\pi/2$  pulse was applied at an off-resonant frequency  $\omega_{\text{off}}$  in order to produce heating effect only, without affecting the NMR line. (b) Corrected relaxation function of nuclear magnetization,  $1 - M(t)_{\text{tot}}/M(t)_{\text{therm}}$ , which is free of heating effect, for three selected temperatures. Solid lines are fits with Eq. (2).

Since  $\sum_q \chi''_{\perp}(q, \omega_0)$  should be the same for both nuclei, the following relation should hold:

$$\frac{^{235}T_1^{-1}}{^{121}T_1^{-1}} = \frac{^{235}(\gamma_n A_{\text{hf}})^2}{^{121}(\gamma_n A_{\text{hf}})^2}, \quad (4)$$

where  $A_{\text{hf}}$  is 5.69 T/ $\mu_B$  for  $^{121}\text{Sb}$  and 147.5 T/ $\mu_B$  for  $^{235}\text{U}$ .<sup>2</sup> Indeed, the experimental values  $^{235}T_1^{-1}$  and  $^{121}T_1^{-1}$  are well scaled according to Eq. (4) above 5 K as shown in the inset of Fig. 4(a). The slight difference between the two data may be due to systematic error from to the *indirect* way of acquiring  $^{235}T_1^{-1}$ . However, we find that  $^{235}T_2^{-1}$  and  $^{121}T_2^{-1}$  data are also scaled with the same ratio between the two  $T_1^{-1}$  data sets at high temperatures. This suggests that the spin fluctuations

dominate both  $T_1^{-1}$  and  $T_2^{-1}$  for the two nuclei. Since both  $T_1^{-1}$  and  $T_2^{-1}$  are scaled with the same ratio, we argue that the slight difference of  $\sum_q \chi''_{\perp}(q, \omega_0)$  may be attributed to an additional contribution to the relaxation rates other than the spin fluctuations, probably, due to the lattice vibrations (phonons) which are not necessarily the same for both nuclei.

In the case that the spin fluctuations dominate,  $T_2^{-1}$  may be written as

$$T_2^{-1} \approx T \gamma_n^2 A_{\text{hf}}^2 \frac{\sum_q \chi''_{\parallel}(q, \omega_0)}{\omega_0} + \frac{1}{2} T_1^{-1} + T_{2,\text{dip}}^{-1}, \quad (5)$$

where  $T_{2,\text{dip}}^{-1}$  is the dipolar term which is estimated to be  $\sim 10^3 \text{ s}^{-1}$  for both  $^{121}\text{Sb}$  and  $^{235}\text{U}$  by summing up the dipolar contribution from the nearest neighbors.<sup>11</sup> In the meantime, we assume that the hyperfine coupling constant  $A_{\text{hf}}$  is isotropic.

For temperatures larger than about 5 K,  $T_1^{-1}$  of both nuclei decreases slowly with decreasing temperature, revealing the  $T^{0.3}$  power law behavior. Below 5 K, however,  $^{121}\text{T}_1^{-1}$  changes abruptly and varies linearly with temperature, yet  $^{235}\text{T}_1^{-1}$  shows no change down to 1.5 K. A similar deviation in the temperature dependence of  $T_2^{-1}$  is observed at 5 K, as shown in Fig. 4 (b), namely  $^{121}\text{T}_2^{-1}$  increases rapidly but  $^{235}\text{T}_2^{-1}$  increases slightly and saturates, with decreasing  $T$ . Interestingly, for U, both nuclear relaxation rates change somewhat with temperature, but for the Sb,  $T_1^{-1}$  decreases and  $T_2^{-1}$  increases below  $\sim 5$  K resulting in the fast increase of the ratio  $T_2^{-1}/T_1^{-1}$  with decreasing  $T$ .

In the ordered antiferromagnetic state,  $T_1^{-1}$  is usually dominated by the fluctuations of the magnetic structure (magnons), in which a two magnon Raman process yields  $T^3$  behavior.<sup>12</sup> Thus, the very small exponent of 0.3 in our case suggests that the relaxation mechanism in  $\text{USb}_2$  is not governed by the simple magnon process. Although the origin of  $T^{0.3}$  behavior is not clear, it suggests that the same relaxation mechanism is applicable to both on-site and ligand nuclear sites.

The clear anomaly of both  $^{121}\text{T}_1^{-1}$  and  $^{121}\text{T}_2^{-1}$  at 5 K in contrast to those of  $^{235}\text{U}$  implies the dramatic change of the hyperfine coupling mechanism for  $^{121}\text{Sb}$ . Since  $A_{\text{hf}}$  for  $^{235}\text{U}$  is expected to be isotropic due to the overwhelming on-site Fermi contact term which is isotropic, the anisotropy of the spin fluctuations above  $\sim 5$  K may be estimated using Eqs. (3) and (5), i.e.,  $\sum_q \chi''_{\parallel} / \sum_q \chi''_{\perp} \sim 18$ . When this ratio is applied for  $^{121}\text{Sb}$ , we obtain  $A_{\text{hf}}^{\parallel} / A_{\text{hf}}^{\perp} \sim 1$ . Therefore,  $A_{\text{hf}}$  is also apparently isotropic for  $^{121}\text{Sb}$  above 5 K. Since the anisotropy of the spin fluctuations does not change much for the  $^{235}\text{U}$ , the anomaly of the relaxation rates of the  $^{121}\text{Sb}$  indicates that the anisotropy of  $A_{\text{hf}}$  is developed below 5 K and the ratio  $A_{\text{hf}}^{\parallel} / A_{\text{hf}}^{\perp}$  increases with decreasing temperature up to 4 at 1.5 K. The anomalous behavior below 5 K may suggest that the hyperfine coupling on the Sb is very sensitive to even a small change of the electronic environment. The

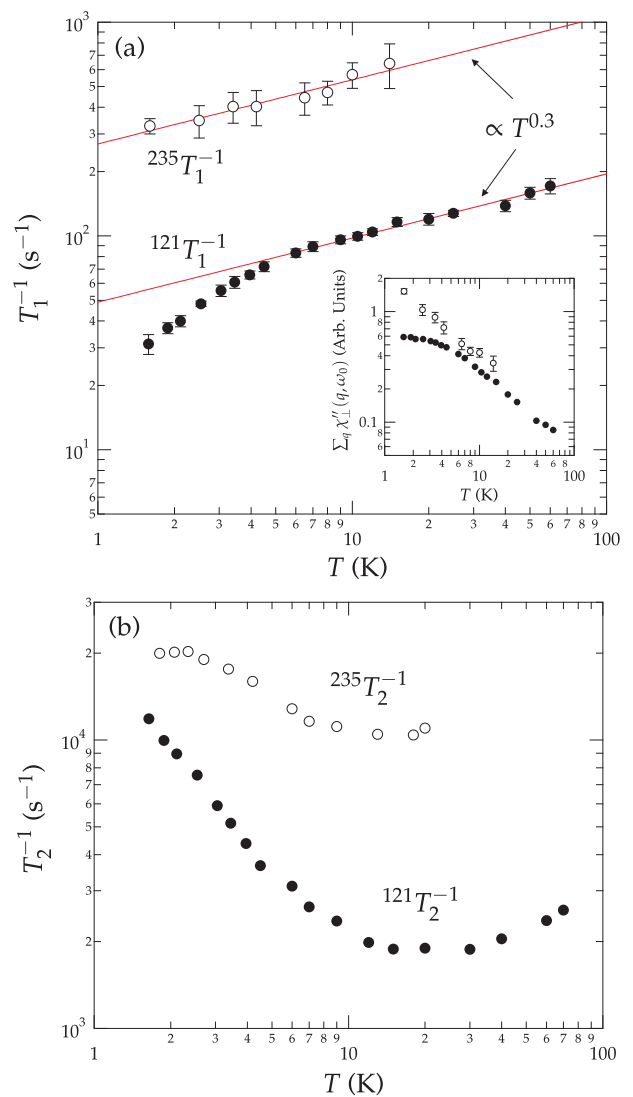


FIG. 4: Nuclear relaxation rates for both  $^{235}\text{U}$  and  $^{121}\text{Sb(I)}$ . (a)  $T_1^{-1}$  as a function of  $T$ . Power law behaviors with the exponent 0.3 were observed. However,  $T_1^{-1}$  of  $^{121}\text{Sb}$  deviates from the power law below 5 K abruptly changing to  $T_1^{-1} \propto T$ . INSET:  $\sum_q \chi''_{\perp}(q, \omega_0)$  vs.  $T$  which reflects the temperature variation of the spin fluctuations. (b)  $T_2^{-1}$  for both nuclei are scaled according to  $(\gamma_n A_{\text{hf}})^2$  exactly as  $T_1^{-1}$  in the high temperature region above 5 K. Below 5 K,  $^{121}\text{T}_2^{-1}$  increases rapidly with decreasing temperature but  $^{235}\text{T}_2^{-1}$  approaches a constant value.

otherwise slight increase of  $^{235}\text{T}_2^{-1}$  below 5 K is then attributed to the cross-relaxation between  $^{235}\text{U}$  and  $^{121}\text{Sb}$ .

#### IV. SUMMARY AND CONCLUSION

The nuclear relaxation rates  $T_1^{-1}$  and  $T_2^{-1}$  of  $^{235}\text{U}$  are reported in the itinerant  $5f$  electron system  $\text{USb}_2$ . The strong heating effect associated with the tiny gyromagnetic ratio of  $^{235}\text{U}$  prevents the direct measurement of

$^{235}\text{T}_1^{-1}$ , but we successfully accounted for the heating effect using two pulse sequences. The resultant  $^{235}\text{T}_1^{-1}$  data as a function of temperature correctly scale according to  $(\gamma_n A_{\text{hf}})^2$  with those of  $^{121}\text{Sb}$ , and vary as  $T^{0.3}$ . We find that  $^{121}\text{T}_1^{-1}$  and  $^{121}\text{T}_2^{-1}$  change dramatically at  $\sim 5$  K, while  $^{235}\text{T}_1^{-1}$  shows no change in the temperature dependence with the slight increase of  $^{235}\text{T}_2^{-1}$ . The different behavior is attributed to the different hyperfine coupling mechanism, but the origin of the anomaly at  $\sim 5$  K is not clear at present. Nevertheless, the successful direct measurement of  $\text{T}_1^{-1}$  on the  $^{235}\text{U}$  in an itinerant compound will pave the way for further direct investiga-

tions of the  $^{235}\text{U}$  nuclei in other U-based compounds.

### Acknowledgment

We thank the useful and delightful discussions with S. Kambe and H. Kato. This work was performed at Los Alamos National Laboratory under the auspices of the US Department of Energy Office of Science and supported in part by the Laboratory Directed Research and Development program.

- 
- <sup>1</sup> K. Ikushima, H. Yasuoka, S. Tsutsui, M. Saeki, S. Nasu, and M. Date, *J. Phys. Soc. Jpn.* **67**, 65 (1998).
- <sup>2</sup> H. Kato, H. Sakai, K. Ikushima, S. Kambe, Y. Tokunaga, D. Aoki, Y. Haga, Y. Ōnuki, H. Yasuoka, and R. E. Walstedt, *J. Phys. Soc. Jpn.* **73**, 2085 (2004).
- <sup>3</sup> G. Amoretti, A. Blaise, and J. Mulak, *J. Magn. Magn. Mater.* **42**, 65 (1984).
- <sup>4</sup> S. Tsutsui, M. Nakada, S. Nasu, Y. Haga, D. Aoki, P. Wiśniewski, and Y. Onuki, *Phys. Rev. B* **69**, 054404 (2004).
- <sup>5</sup> Z. Henkie, R. Maslanka, P. Wisniewski, R. Fabrowski, P. Markowski, J. Franse, and M. van Sprang, *J. Alloys Compd.* **181**, 267 (1992).
- <sup>6</sup> S. Lebègue, P. M. Oppeneer, and O. Eriksson, *Phys. Rev. B* **73**, 045119 (2006).
- <sup>7</sup> J. Leciejewicz, R. Troć, A. Muraśnik, and A. Zygmunt, *phys. status solidi (b)* **22**, 517 (1967).
- <sup>8</sup> D. Aoki, P. Wiśniewski, K. Miyake, N. Watanabe, Y. Inada, R. Settai, E. Yamamoto, Y. Haga, and Y. Ōnuki, *J. Phys. Soc. Jpn.* **68**, 2182 (1999).
- <sup>9</sup> E. Guziewicz, T. Durakiewicz, M. T. Butterfield, C. G. Olson, J. J. Joyce, A. J. Arko, J. L. Sarrao, D. P. Moore, and L. Morales, *Phys. Rev. B* **69**, 045102 (2004).
- <sup>10</sup> T. Moriya, *J. Phys. Soc. Jpn.* **18**, 516 (1963).
- <sup>11</sup> A. Abragam, *The Principles of Nuclear Magnetism* (Oxford University Press, 1961).
- <sup>12</sup> V. Jaccarino, in *Magnetism IIA*, edited by G. Rado and H. Suhl (Academic Press, New York, 1966).